

# RADIATION LOAD STUDIES FOR THE FCC-ee POSITRON SOURCE WITH A SUPERCONDUCTING MATCHING DEVICE\*

B. Humann<sup>†1</sup>, A. Lechner, Y. Zhao, A. Latina, CERN, Geneva, Switzerland  
B. Auchmann, J. Kosse, PSI, Villingen, Switzerland  
I. Chaikovska, S. Ogur, CNRS/IN2P3, Orsay, France  
<sup>1</sup>also at TU Wien, Vienna, Austria

## Abstract

For an electron-positron collider like the Future Circular Collider lepton machine (FCC-ee), the production of positrons plays a crucial role. One of the design options considered for the FCC-ee positron source employs a superconducting solenoid made of high temperature superconductor coils as an adiabatic matching device. The solenoid, which is placed around the production target, is needed to capture positrons before they can be accelerated in a linear accelerator. A superconducting solenoid yields a higher peak field than a conventional normal-conducting matching device, therefore increasing the achievable positron yield. In order to achieve an acceptable positron production, the considered target is made of tungsten-rhenium, which gives also a significant flux of unwanted secondary particles, that in turn could generate a too large radiation load on the superconducting coils. In this study, we assess the feasibility of such a positron source by studying the heat load and long-term radiation damage in the superconducting matching device and surrounding structures. Results are presented for different geometric configurations of the matching device.

## INTRODUCTION

The Future Circular Collider lepton machine (FCC-ee) is one option for a new collider at CERN [1]. With a circumference of around 91 km it is meant to store and collide electrons and positrons with different beam energies ranging from 45.6 GeV to 182.5 GeV. The different operation modes enable precision measurements over a wide energy range, spanning from the  $Z$  pole to the  $t\bar{t}$  threshold. Operation relies on the production of high-intensity and low-emittance positron beams, both for filling the collider when empty and for top-up injection. [2]. Positron sources typically use an adiabatic matching device for capturing positrons from a heavy target before they can be accelerated in a first linear accelerator. The baseline solution considered for FCC-ee assumes a classical magnetic matching device consisting of a tapered normal-conducting solenoid downstream of the target [3]. The entire assembly is further enclosed by bridge coils. A similar solution is already used for the positron source at SuperKEKB [4]. As a novel alternative for FCC, a superconducting solenoid made of YBCO tapes is considered. Using a superconducting matching device allows for higher magnetic field, which in turn enables a higher

positron yield. A demonstrator of such a high-temperature superconductor (HTS)-based positron source, called P<sup>3</sup>, will be built at the SwissFEL facility at PSI [5].

Although a superconducting matching device is beneficial for the positron yield, it exhibits a higher sensitivity to radiation. In this paper, we present first radiation load studies for a FCC-ee positron source with HTS coils. The studies were carried out with the FLUKA Monte Carlo code [6–8], which is commonly used for shielding calculations. We consider two different configurations with different coil and beam apertures, one being similar to the P<sup>3</sup> experiment [5], whereas the second layout has a larger vacuum chamber. For both configurations, we quantify the instantaneous power deposition and the cumulative radiation damage. The results are scaled to collider operation at the  $Z$  pole (45.6 GeV), which requires the highest positron intensity [1]. The assumed electron drive beam has an energy of 6 GeV and a beam spot size of 0.5 mm rms at the target. The repetition rate lies at 200 Hz, with a electron bunch charge of 1.43 nC and two bunches per pulse, which leads to a drive beam power of 3.43 kW [9]. This beam power is needed when refilling the collider when empty, but is around one order of magnitude less during top-up injection [1].

## SIMULATION SETUP

In this study, a conventional target configuration is considered (see Fig. 1), where the electron drive beam directly impacts on a disk made of tungsten-rhenium alloy. When the electrons enter the target, they emit electromagnetic radiation in the form of Bremsstrahlung photons. The produced photons are then subject to electron-positron pair production. These two processes happen in form of a cascade, as long as the energy is high enough. After the target, photons, electrons and positrons can be found. An alternative production scheme under consideration for the FCC-ee is based on a hybrid setup [3], where the electron beam first generates photons through coherent interaction with a crystal; the photons then impact on a target, where positrons are produced. However, this alternative scheme is not considered here. The target thickness is selected to be  $5X_0$  (17.5 mm), with  $X_0$  being the radiation length. The target thickness has been optimised for the positron yield in a separate study [10]. The engineering and cooling design of the target, as well as the target integration inside the cryostat are beyond the scope of this paper. We therefore consider a simple stationary disk.

In the following, two different versions of the matching device are discussed (see Fig. 2), that have similar gross

\* Work supported by FCC.

<sup>†</sup> barbara.humann@cern.ch

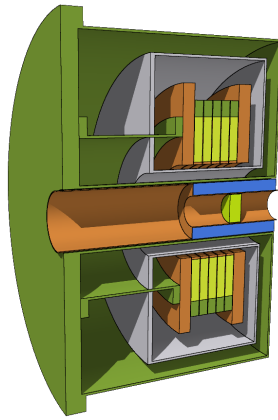


Figure 1: 3D cut of the geometry.

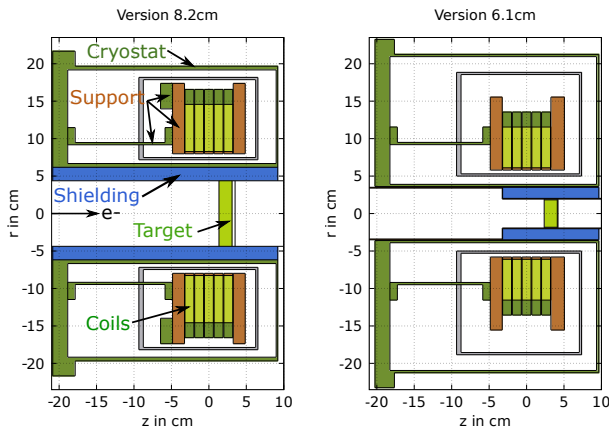


Figure 2: Positron production source geometry.

features, but different bore apertures, shielding thicknesses. While the shape of the magnetic fields is slightly different for the two versions, the peak value is the same ( $B_{max} = 20$  T). The versions are called  $V_{8.2cm}$  and  $V_{6.1cm}$ , with the numbers giving the radius at which the magnet coils are located. Both versions have 5 coils made out of YBCO tapes. The coils are supported by a copper/stain-less steel structure, which is embedded in a stainless steel cryostat. The target is surrounded by a shielding made of Inermet-180®, a tungsten alloy, which reduces the radiation load to the cryostat and coils. The shielding extends over the whole cryostat length for  $V_{8.2cm}$ , while it starts at the first coil for  $V_{6.1cm}$ . The beam aperture inside the shielding is about 4.4 cm for  $V_{8.2cm}$  and about 1.9 cm for  $V_{6.1cm}$ . Additionally, two different target positions were considered for  $V_{6.1cm}$ , corresponding to the optimal positions (maximum yield) for either a L-band or a S-band capture Linac. In the first case, the target exit is located 4.1 cm downstream from the peak field and in the second case the distance is 2 cm. In  $V_{8.2cm}$  the target exit is located at 3.1 cm.

## POWER DEPOSITION

Table 1 shows the total absorbed power in the target, shielding, cryostat and coils, for a drive beam power of

Table 1: Absorbed Power in Different Components

	$V_{8.2cm}$	$V_{6.1cm}$ L-band	$V_{6.1cm}$ S-band
Target	906 W	862 W	869 W
Shielding	69 W	149 W	209 W
Cryostat and coil supports	3.3 W	8.1 W	11.8 W
Coils (1-5)	0.09 W to 0.18 W	0.15 W to 0.68 W	0.27 W to 1.25 W
<b>Total</b>	<b>980 W</b>	<b>1030 W</b>	<b>1126 W</b>

3.43 kW. Figure 3 provides a global overview of the corresponding power density distribution in the entire setup.

The results indicate that about one quarter of the electron beam power is dissipated in the target. The heat load in the target is somewhat higher in  $V_{8.2cm}$  because of its larger radius (4.4 cm) compared to  $V_{6.1cm}$  (1.8 cm). The peak power density at the target exit face reaches up to  $21 \text{ kW/cm}^3$  in all cases (note that Fig. 3 does not resolve the peak power density in the target due to the coarse scoring mesh used in this figure). The total power deposition in the Inermet-180 shielding reaches between  $\sim 70$  W ( $V_{8.2cm}$ ) and  $\sim 210$  W ( $V_{6.1cm}$ , S-band). The power load is higher in the latter version due to the smaller aperture. Dedicated thermo-mechanical studies are needed to develop an engineering solution, which copes with the heat load in target and shielding. Although the total heat load and the peak power density is significant, it is not excluded that the actual target can be stationary.

Evaluating the heat load on the HTS coils is critical for assessing the feasibility of a superconducting matching device. As shown in Table 1, the total power deposition in the most exposed coil ranges from  $\sim 0.2$  W ( $V_{8.2cm}$ ) to  $\sim 0.7$  W/1.25 W ( $V_{6.1cm}$ , L-band/S-band). The results are lower for  $V_{8.2cm}$  due to several reasons. First, the coils are less impacted due to their position at a larger radius compared to the other version. Secondly, the shielding for  $V_{8.2cm}$  is slightly thicker (1.8 cm) compared to  $V_{6.1cm}$  (1.4 cm). The results also show that the longitudinal position of the target inside the cryostat has a non-negligible impact on the power deposition in the coils. Comparing the results of the L-band and the S-band option (both  $V_{6.1cm}$ ) shows that a 2 cm shift can almost double the total power in the coils. The peak power density in the coils ranges from  $1 \text{ mW/cm}^3$  for  $V_{8.2cm}$  to up to  $16 \text{ mW/cm}^3$  in the S-band version of  $V_{6.1cm}$ . The L-band option (not shown in the figure) has a maximum value of about  $8 \text{ mW/cm}^3$ . Both the observed power densities and the total power deposition in the coils are considered acceptable, i.e. values are below the quench level and are compatible with the heat extraction capacity of the cryogenic system.

Depending on the geometry around 2.3 kW-2.45 kW are escaping the matching device, which corresponds to 67-71% of the total power. About 1.98 kW of this power is carried by photons and electrons, which are strongly concentrated around the beam axis of the original electron drive beam.

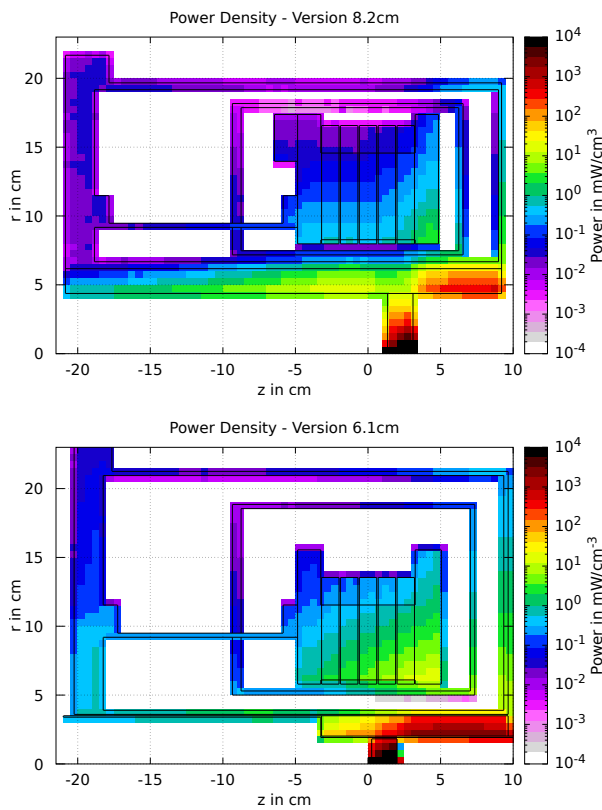


Figure 3: Power density distribution in the target, shielding, cryostat and coils (top:  $V_{8.2\text{cm}}$ , bottom:  $V_{6.1\text{cm}}$ , S-band)

With this localised distribution, the impact on the downstream beam line has to be studied thoroughly to assess the shielding requirements.

### CUMULATIVE RADIATION EFFECTS

The investigated quantities related to long-term radiation effects are the ionising dose that may cause a deterioration of material properties, especially in organic materials [11], and the Displacement Per Atom (DPA), which is responsible for the structural damage of inorganic materials [12]. We provide estimates of these quantities for one year of operation at the Z pole. We assume that the collider is filled twice a day, during which a maximum electron drive beam power (3.43 kW) is needed. The filling time is estimated to last

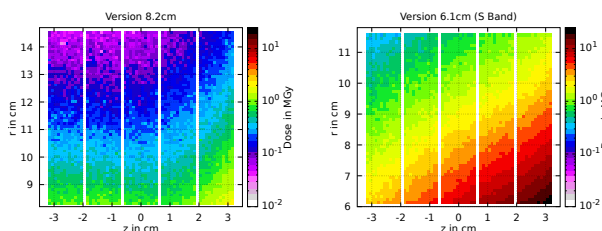


Figure 4: Dose distribution in the HTS coils for 1 year of operation at the Z pole (left:  $V_{8.2\text{cm}}$ , right:  $V_{6.1\text{cm}}$ , S-band)

2.4% of the total operational time [1]. We further assume that during the rest of the time the collider will be in top-up injection mode, which requires a lower bunch charge and hence a lower drive beam power (about 10% of the maximum). In total, the machine will be four years in Z operation, followed by 10 years at various higher beam energies, but with a significantly reduced beam current [1]. The operating conditions of the positron source for the other operation modes still have to be established, but we conservatively assume that a factor of  $\sim 10$  has to be applied to the obtained numbers to quantify the cumulative dose and DPA for the full collider lifetime.

Figure 4 presents a detailed view of the dose distribution in the five coils. In the larger-aperture version  $V_{8.2\text{cm}}$  the integrated dose goes up to 2 MGy/year. The highest dose levels are observed in the S-band case of  $V_{6.1\text{cm}}$ , where a maximum of 22 MGy/year is reached, while for the L-band version, the dose reaches 8 MGy/year. Scaled to the full collider lifetime, the dose values in  $V_{6.1\text{cm}}$  reach excessive values. These values would not be compatible with any organic insulation or support materials. The HTS coils can, however, be manufactured without any organic insulation. Nevertheless, possible effects of the high dose on the superconductor need to be further assessed. In any case, the dose values can be well reduced by choosing a larger aperture, as in version  $V_{8.2\text{cm}}$ .

The simulation shows that the cumulative displacement damage in the tungsten-rhenium target reaches up to 3 DPA/year (here a damage threshold of 90 eV was assumed). This estimate neglects any annealing effects resulting from the elevated temperature of the target during source operation. The found value is not negligible and the effects on the target properties have to be assessed. Potentially, the target needs to be exchanged throughout the years or other measures might be required (e.g. exposing a fresh surface of the target after a certain operating period). The DPA in the coils is much lower, which is expected due to their peripheral position. For  $V_{8.2\text{cm}}$  the maximum DPA is found to be around  $2 \times 10^{-5}$  DPA/year, while for  $V_{6.1\text{cm}}$  (S-band) it reaches up to  $1 \times 10^{-4}$  DPA/year. The long term effects of the DPA on the material have to be further investigated. Due to the different target position, the S-band version is again stronger impacted than the L-band version.

### CONCLUSION

This paper presented first radiation load studies for the FCC-ee positron source with a superconducting matching device. Two different configurations with different coil apertures (6.1 cm and 8.2 cm) were compared. In both cases, the cryostat and coils were shielded by a thick tungsten absorber. While the power load to the superconducting coils and cryostat appears acceptable in both cases, high cumulative dose values are found for the smaller aperture version. Nevertheless, it has been shown that a superconducting matching device for the positron production target is feasible and no showstoppers have been identified.

## REFERENCES

- [1] A. Abada *et al.*, “FCC-ee: The Lepton Collider,” *Eur. Phys. J. Spec. Top.*, vol. 228, pp. 261–623, 2019, doi:10.1140/epjst/e2019-900045-4
- [2] M. Aiba *et al.*, “Top-up injection schemes for future circular lepton collider,” *Nucl. Instrum. Methods Phys. Res. B*, vol. 880, pp. 98–106, 2018, doi:10.1016/j.nima.2017.10.075
- [3] I. Chaikovska *et al.*, “Positron Source for FCC-ee,” in *Proc. 10th International Particle Accelerator Conference (IPAC’19), Melbourne, Australia*, 2019, pp. 424–427, doi:10.18429/JACoW-IPAC2019-MOPMP003
- [4] L. Zang, S. Fukuda, T. Kamitani, and Y. Ogawa, “Design optimization of flux concentrator for SuperKEKB,” in *Proc. 3rd International Particle Accelerator Conference (IPAC’12), New Orleans, LA, USA*, 2012, pp. 1473–1475, doi:10.18429/JACoW-IPAC2019-MOPMP003
- [5] N. Vallis *et al.*, “The PSI Positron Production Project,” presented at LINAC’22, Liverpool, United Kingdom, Aug. 2022, unpublished.
- [6] G. Battistoni *et al.*, “Overview of the FLUKA code,” *Annals of Nuclear Energy*, vol. 82, pp. 10–18, 2015, Joint International Conference on Supercomputing in Nuclear Applications and Monte Carlo 2013, SNA + MC 2013., doi:10.1016/j.anucene.2014.11.007
- [7] C. Ahdida *et al.*, “New capabilities of the FLUKA multi-purpose code,” *Front. Phys.*, vol. 9, 2022, doi:10.3389/fphy.2021.788253
- [8] *FLUKA.CERN website*, <https://fluka.cern/>.
- [9] P. Craievich *et al.*, “The FCC-ee Pre-Injector Complex,” presented at IPAC’22, Bangkok, Thailand, Jun. 2022, paper WEPOPT063, this conference.
- [10] Y. Zhao *et al.*, “Comparison of Different Matching Device Field Profiles for the FCC-ee Positron Source,” in *Proc. IPAC’21*, 2021, pp. 2617–2620, doi:10.18429/JACoW-IPAC2021-WEPAB015
- [11] N. Mokhov *et al.*, “Energy deposition studies for the high-luminosity Large Hadron Collider inner triplet magnets,” *Phys. Rev. ST Accel. Beams*, vol. 18, p. 051001, 2015, doi:10.1103/PhysRevSTAB.18.051001
- [12] R. Flükiger *et al.*, “Variation of Tc, lattice parameter and atomic ordering in Nb3Sn platelets irradiated with 12 MeV protons: Correlation with the number of induced Frenkel defects,” *Superconductor Science and Technology*, vol. 30, 2017, doi:10.1088/1361-6668/aa64ee